Measuring Effects of Refractive Surgery On Corneas Using Taylor Series Polynomials

Jacob A. Corbin[a,b], Stanley Klein[c], and Corina van de Pol[c]

[a]Neurometrics Institute, Berkeley, CA 94704
[b]University of California at Santa Cruz, Santa Cruz, CA 95064
[c]University of California at Berkeley, Berkeley, CA 94720

ABSTRACT

Corneal topographers have made it possible to accurately map corneal shape. We applied this technology to model the post-refractive surgery cornea using Taylor series polynomials. Topography data was taken from 58 patient eyes with photorefractive keratectomy (PRK) or astigmatic photorefractive keratectomy (PARK). We looked at the changes the cornea underwent surgically, as well as the healing process. We compared the post-ablation cornea to the pre-ablation cornea and to the intended correction using novel topography maps. From the refractive map, we quantified the spherical aberration as areas of defocus on the cornea.

From the pre-op exam to the first post-op exam, we measured 0.19 ± 0.10 mm radius decrease in PRK, and a 0.13 ± 0.08 mm radius decrease in PARK in the areas where rays come to within two diopters of defocus. As this change occurs within the optical zone, this corresponds to an increase in spherical aberration for both the PRK and the PARK patient. As the patient healed, we found additional decrease in radius of the zones of best vision in PRK patients, whereas we found no significant decrease in PARK patients. This corresponds to increased spherical aberration in the PRK patient.

Keywords: aberration, cornea, corneal modeling, corneal topography, PARK, PRK, refractive map, spherical aberration, Taylor series, Zernike polynomials

1. INTRODUCTION

Photorefractive keratectomy (PRK) and astigmatic photorefractive keratectomy (PARK) are two similar procedures that ablate a thin layer of the cornea, changing the cornea's refractive power, intending to eliminate the need for spectacles or contact lenses. The PARK procedure also corrects astigmatism. While these procedures have done well in correcting refractive error, it has come at the cost of visual acuity and contrast sensitivity, especially in low light conditions where the pupil is wide[1-3]. Loss of acuity is at least partially due to the introduction of spherical aberration from these procedures[4-5]. Spherical aberration is a discrepancy in the focal length from the center to the periphery of a lens. Spherical aberration is illustrated in figure 1, where the peripheral rays focus at a different point than the central rays. As the pupil size increases, spherical aberration becomes more pronounced, which accounts for problems in low lighting where the pupil is dilated.

Figure 1- Spherical aberration: Incoming parallel rays on the lens (gray) have different focal lengths. Peripheral rays (dashed) come to focus at point 1, while central rays (solid) come to focus at point 2.

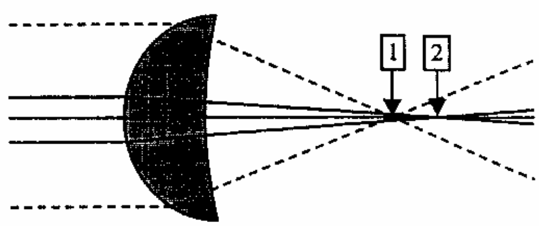

Previous studies using a corneal topographer[4] and a Hartmann-Shack wavefront sensor[5] suggest an increase in spherical aberration after PRK surgery. Our team set out to verify these findings using data acquired from corneal topographers and by using a novel method of analyzing this data using a Taylor series expansion. We also measured the time course of the development of spherical aberration to determine whether introduction of aberrations was immediate after the surgery or whether it was a slow process related to the regrowth of the epithelium.

Part of the SPIE Conference on Ophthalmic Technologies IX • San Jose, California • January 1999
SPIE Vol. 3591 • 0277-786X/99/$10.00

2. METHODS

2.1 Development of Taylor Series Shape Descriptors

The axis is placed with the corneal vertex at the origin, and the eye looking in the –z direction, as shown in figure 2.

Figure 2 – the corneal alignment with axes

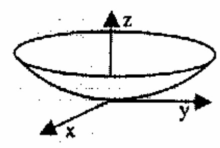

A modification of the Taylor series expansion in x and y similar to a Zernike polynomial series for an arbitrary query for the height is used (for simplicity, it is shown here as equation (1) in cylindrical coordinates, r, θ, z).

$$z = \mathrm{Re}\left(\sum_{n=m=0}^{n=m=10} \mathrm{Coef}_{nm}\ r^n\ e^{im\theta} \right) \tag{1}$$

In this study, we used n_{max} and $m_{max} = 10$ for a total of 66 coefficients (36 complex coefficients). These coefficients provide a concise description of the corneal shape. Calculations were performed using Matlab® (MathWorks, MA).

The Taylor expansion that we used gives an identical fit to the corneal shape as that which would be obtained using Zernike polynomials or a Taylor's series of terms of the form $x^a\ y^b$ where a+b=n. The advantage of our expansion is that the low order terms have clinical relevance. The coefficient with n=2 and m=0 (a real number) corresponds to the <u>paraxial</u> mean sphere. The coefficient with n=2 and m=2 (a complex number) corresponds to the paraxial toricity, with the magnitude of the coefficient being the magnitude of the paraxial toricity and the phase angle being the angle of the toricity. For the Zernike expansion the corresponding coefficients are averages of the sphere and toricity across the entire cornea contributing to the fit, rather than being the values at the axis. An alternative to using the Taylor expansion would be to use a spline expansion. The spline has the advantage of having a larger radius of convergence and possibly less ringing. But typical splines have the disadvantage that they impose a rectangular structure to what is essentially a radial fitting situation. Further study is needed for determining the optimal basis set to be used for fitting normal and anomalous corneas.

2.2 Derivation of Topography Maps

Because the first and second derivatives of z can be found analytically in the x and y directions, this provides an accurate method of finding other qualities of the corneal surface at an arbitrary point. These properties include the normal, the maximum and minimum curvature, and the maximum and minimum curvature directions. It is straightforward to then find other maps, such as the (meridional) axial curvature, meridional power (previously called instantaneous curvature), gaussian curvature, and the mean instantaneous curvature. Important for this study, we can also find the refractive map.

2.2.1 The refractive map

The refractive map is defined in diopters as: 1.3375/f, the index of refraction divided by the secondary focal length, f. The index of refraction for an average cornea is 1.3375. The secondary focal length (figure 3) is the distance from the corneal

Figure 3 - Secondary Focal Length

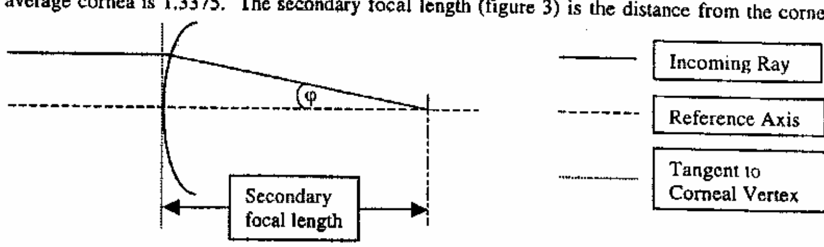

vertex to the intersection of a refracted incoming parallel ray with the reference axis[6]. To compute the secondary focal length for any point on the cornea, one needs to know the sagittal (sag) height, and the normal on the cornea at this point. The sag height is the z coordinate of the cornea at the point of interest, as in figure 2. The ray is traced using Snell's Law until it intersects with the reference axis. The secondary focal length given by:

$$f = z + r / \tan \varphi \qquad (2)$$

Where z is the sag height, r is the distance of the point in question to the reference axis, and φ is the angle the incoming ray makes with the reference axis. Of course on a typical cornea, one would not expect too many incoming rays to intersect the reference axis at all! Two methods can be employed. One method is to find the point where a ray gets closest to the reference axis. The method we used is to apply Snell's Law in the meridional plane. The refracted ray is then constrained to intersect the axis.

Figure 4 - The refractive map of a post-PRK cornea with the one, two, and three diopter areas of aberration overlaid.

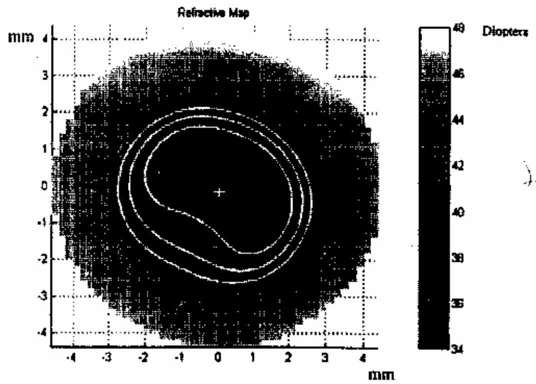

2.2.2 Using the refractive map to find spherical aberration on the cornea

The refractive map (figure 4) can be used to find spherical aberration. A reference paraboloid is made using our Taylor series polynomials, using the coefficients $C_{2,0}$ and $C_{2,2}$, which is just the lens's refractive power and astigmatism and the refractive map of this paraboloid is found. Subtracting the cornea's refractive map with this reference paraboloid will give us a difference map in units of diopters of spherical aberration out of focus. The center of the difference map is near zero diopters, and the difference map shows the cornea's aberrations. Finding the areas where the cornea is one, two and three diopters out of focus is similar to mapping the difference map like a contour map. The graphical results are the three white rings overlaid on top of figure 4, the innermost being the one diopter zone while the outermost being the three diopter zone. Another way of looking at this difference map is that we are removing the most powerful terms of the Taylor series, leaving the aberrations.

2.3 Application to a Cornea after Refractive Surgery

2.3.1 Intended ablation

An unablated cornea's curvature should be close to flat, and ideally it should decrease slightly as one moves away from the center. For simplicity, the pre-operative curvature is drawn as a flat line in figure 5. After sugery, the curvature in the optic zone should remain close to flat. For both the PRK and PARK procedures, the power is changed in the optic zone (usually reduced), bringing the focal point of the rays that enter the optic zone onto the retina. A small transition zone is created between the ablated section and the unablated sections. Without this transition zone, there would be a very sharp discontinuity between the ablated and the unablated sections (a sharp edge). The radius of the optic zone is 2.75 mm for the Nidek laser used in the present study.

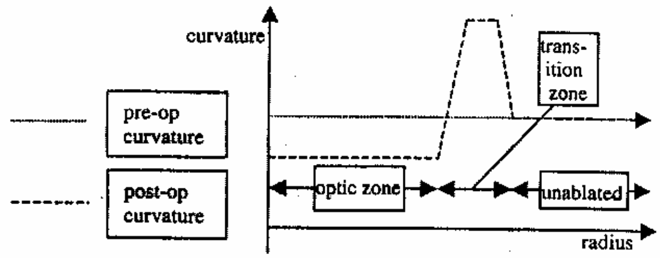

Figure 5- Radial Curvature on the Cornea Before and After Refractive Surgery

2.3.2 Data collection

The data was collected for use in the FDA phase III trial for the NIDEK scanning laser system. Measurements were taken at pre-op, and 1, 3, 6, 9, 12, 18, and 24 months post-operatively as required by the FDA study. All but two patients had PRK or PARK completed at the Beckman Vision Center, University of California San Francisco, by one of three refractive surgeons. The total number of eyes evaluated is 58. Patient demographics are summarized in Table 1.

Table 1: Patient Demographics

Procedure	Eyes (Total=58)	Age (sd)	M/F	Pre-op spherical equivalent (sd)	Pre-op cylinder (sd)
PRK	25	40.6 (10.2)	40% M 60% F	-7.5 Diopters (2.09)	0.4 Diopters (0.312)
PARK	33	47.6 (9.9)	36% M 64% F	-5.8 Diopters (1.50)	1.5 Diopters (0.878)

Measurements were taken using the Tomey® TMS-2 (Computed Anatomy, New York, NY) corneal topographer. The sag height and the radius measurements for each ring were exported from the TMS-2 for further analysis. Subjects who elected for the PARK procedure have more cylinder than subjects who elected for the PRK procedure, as PARK also attempts to correct for astigmatism.

3. RESULTS

3.1 Initial observations

Before quantifying our findings, we made visual inspections of the meridional curvature of the postrefractive surgery patients. Surprisingly, a typical meridian might look like figure 6, where we see an increase in curvature before the beginning of the transition zone, shown here as the vertical line at 2.75 mm. The intended ablation is shown here as the dashed line. Increasing curvature as one moves away from the cornea's center indicates spherical aberration introduced by the surgery. This corresponds to an oblate cornea, whereas pre-PRK corneas are prolate.

Figure 6 - Increasing curvature before the beginning of the transition zone indicates spherical aberration being introduced into the eye. Dashed line represents intended curvature.

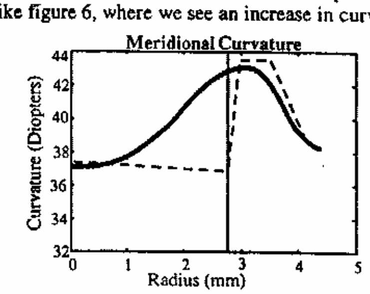

We would like to know if this spherical aberration is introduced in the surgery, or as part of the healing process. The pre-operative cornea is compared to the first available post-operative exam, and also compared the first available post-operative exam with the same patients' last available post-operative exam.

3.2 Radius of Area of Best Vision, From Pre-Op to First Post-Op

The first metric is the increase in spherical aberration from the pre-operative cornea to the first available post-operative cornea. Comparisons were made between the areas of one, two, and three diopters of aberration (section 2.2.2) of each patient's pre-operative exam to their first available prost-operative exam, and then converted to the change in average radius (average radius = $(\text{Area}/\pi)^{1/2}$) for these three zones. The post-op data was the first available post-op data, which was usually three months, but the one month examination was used when available. The average first post-operative was 2.6 ± 2.2 months for PRK and 2.4 ± 1.6 months for PARK (months ± standard deviation).

Table 2 – Pre-Op to First Post-Op Decrease of Radius of Zone of Defocus ± std err		
	PRK (n=19)	PARK (n=29)
1 diopter zone decrease (mm)	-0.08 ± 0.09	-0.04 ± 0.09
2 diopter zone decrease (mm)	0.19 ± 0.10	0.13 ± 0.08
3 diopter zone decrease (mm)	0.50 ± 0.12	0.32 ± 0.09

Table 2 shows the decrease in the average radius for the three zones. For both PRK and PARK patients, we can see there is no significant change in the one diopter zone. This is to be expected, as this should correlate to the centermost part of the eye, close to where we are defining the change to be zero. It was a surprise that our results leaned toward an increase in radius, albeit insignificant. The two diopter zone is our main result and the most telling. For both PRK and PARK, these areas decreased quite significantly, which correlates to an increase in spherical aberration. The three diopter zone was, for the most part, out of the optical zone, so these results are irrelevant because changes are expected in the transition zone. Figure 7 shows the same data, presented as correlation graphs of the pre-op to post-op for PRK and PARK. The horizontal and vertical lines represents the limit of the optical zone as predefined by the Nidek laser.

Figure 7 - Comparison of Post-op radius of Best Vision to Pre-op Radius of Best Vision

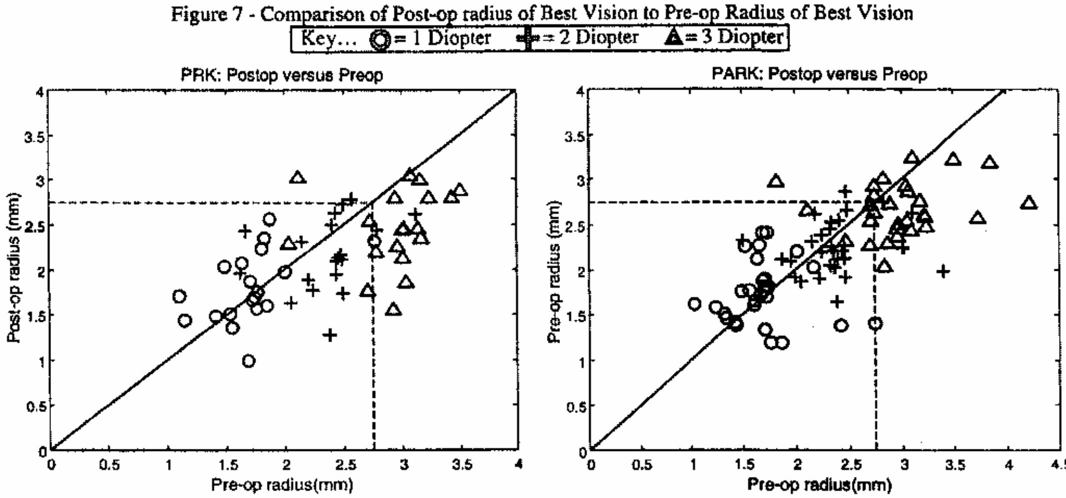

The graphs in figure 7 are divided by the diagonal lines radius pre-operative = radius post-operative. Points above this line indicate a decreased in aberrations, while points below this line indicate an increase in aberrations. As indicated by the key, circles indicate one, plus-signs two, and triangles are three diopters of aberration, relating to the number of sides or segments of each shape.

3.3 Radius of Area of Best Vision, From Three Months to Nine Months

Using the same technique as the previous section, the healing process was studied. Comparing the areas of defocus (section 2.2.2) of the three month post-operative exam to the last available exam, there was evidence of an increase of spherical aberration. Again referring to figure 4, which shows the refractive map, there are three areas shown as three overlaid white rings. If spherical aberration increases with the healing process, these areas will decrease in average radius. The last available patient exams varied from six months to eighteen months, but averaged 8.8 ± 2.5 months for PRK and 9.1 ± 2.3 months for PARK.

Table 3 – Three Month Exam to Last Available Exam
Radial Decrease in Best Vision Areas (mm) ± std err

	PRK (n=25)	PARK (n=33)
radius decrease, 1 diopter (mm)	0.11 ± 0.06	0.01 ± 0.08
radius decrease, 2 diopter (mm)	0.09 ± 0.06	-0.01 ± 0.06
radius decrease, 3 diopter (mm)	0.07 ± 0.07	0.02 ± 0.04

Table 3 shows the decrease in the average radius for the three zones. Our results indicate that the healing process produces no significant change in the cornea for PARK. This time, with the healing process, we see a decrease in the areas of best vision for PRK for both the one and the two diopter zones, and no significant change in the three diopter zone. The decrease in the three diopter zone was small, and bordering on insignificant. Again, the three diopter zone is typically beyond the optical zone, and so it is unimportant where vision is concerned. Figure 8 shows this same data as a correlation graph.

Figure 8 – The Healing Cornea, From Three Months to Nine Months

Key... O = 1 Diopter + = 2 Diopter Δ = 3 Diopter

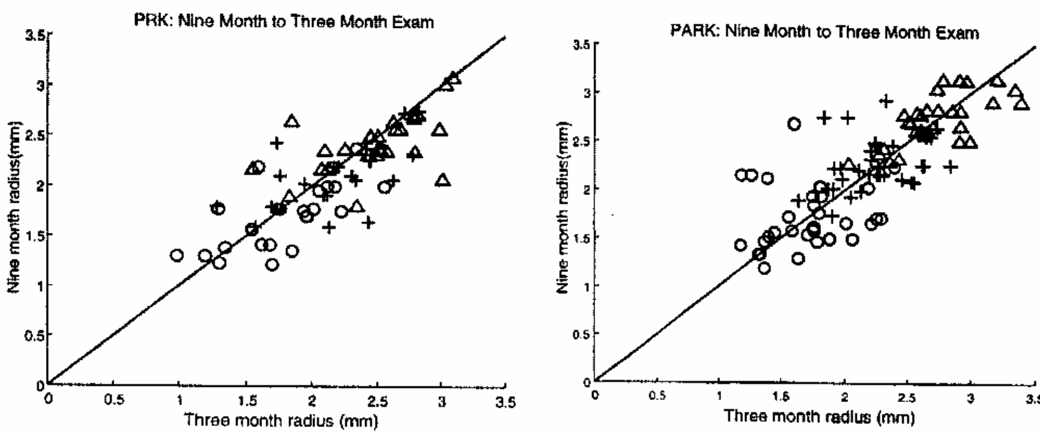

4. DISCUSSION

The findings verified increased spherical aberrations in the cornea following refractive surgery, quantifying the increase of the spherical aberration as an encroachment of increased power. It should be noted that the correction of –7.5 diopters for the PRK group and -5.8 diopters for the PARK group is large.

Studies suggest that regression of correction in PRK corneas is due to the epithelial regrowth after surgery[7-9]. Another study found the epithelium to be 24% thicker in the central zone than the patients' unablated control eye when using an excimer laser that has a similar radius of ablation to the Nidek[10]. The role of the epithelium seems to be to smooth the cornea out as much as possible. If, after PRK, the epithelium were to grow back evenly, there should be minimal regression. However, to smooth the cornea as much as possible, the epithelium should grow thickest at the center, and grow thinner until it meets the sharp transition zone. Not only should the power regress, as it is found to do, but also spherical aberration would be introduced.

ACKNOWLEDGMENTS

This study was supported by NIH grant #R44-11211. The authors are grateful to Thom Carney, John Corzine, and to Fergal Shevlin for proofreading and insight.

REFERENCE

1. A. Ghaith, J. Daniel, et al., "Contrast Sensitivity and Glare Disability After Radial Keratotomy and Photorefractive Keratectomy", *Arch Ophthalmol*, Vol 116: 12-18, 1998.
2. W. Verdon, M. Bullimore, R. Maloney, "Visual Performance After Photorefractive Keratectomy", *Arch Ophthalmol*, Vol 114: 1465-1472, 1996.
3. U. Niesen, U. Businger, et al., "Glare Sensitivity and Visual Acuity After Excimer Laser Photorefractive Keratectomy for Myopia", *Br J Ophthalmology*, 81: 136-140, 1997.
4. K. Oliver, R. Hemenger, et al., "Corneal Optical Aberrations Induced by Photorefractive Keratectomy", *J Ref Surgery*, 13: 246-254, 1997.
5. M. Campbell, "Contributions to Image Quality in the Eye", *14th Interdisciplinary Laser Science Conference, OSA*, MAA1, 69, 1998.
6. S. Klein and R. Mandell, "Shape and Refractive Powers In Corneal Topography", *IVOS*, Vol 36, No 10:2096-2109, 1995.
7. C. Gauthier, B. Holden, D. Epstein, et al., "Role of Epithelial Hyperplasia in Regression Following Photorefractive Keratectomy", *Br J Ophthalmology* 80:545-548, 1996.
8. T. Møller-Pedersen, M. Vogel, et al., "Quantification of Stromal Thinning, Epithelial Thickness, and Corneal Haze after Photorefractive Keratectomy Using In Vivo Confocal Microscopy", *Ophthalmology*, 104:3 360-368, 1997.
9. P. Fagerholm, H. Hamberg-Nyström, B. Tengroth, "Wound Healing and Myopic Regression Following Photorefractive Keratectomy", *ACTA Ophthalmologica*, 72: 229-234, 1994.
10. C. Gauthier, D. Epstein, B. Holden, et al., "Epithelial Alterations Following Photorefractive Keratectomy for Myopia", *J Ref Surgery* 11:113-118, 1995.